

DETECTION TIME FOR PLAUSIBLE CHANGES IN ANNUAL PRECIPITATION, EVAPOTRANSPIRATION, AND STREAMFLOW IN THREE MISSISSIPPI RIVER SUB-BASINS

ALAN D. ZIEGLER¹, EDWIN P. MAURER², JUSTIN SHEFFIELD¹, BART NIJSSEN³,
ERIC F. WOOD¹ and DENNIS P. LETTENMAIER⁴

¹*Environmental Engineering & Water Resources,
Princeton University, Princeton, New Jersey, U.S.A.*

E-mail: adz@princeton.edu

²*Department of Civil Engineering, Santa Clara University, Santa Clara, California, U.S.A.*

³*Departments of Civil Engineering & Engineering Mechanics and Department
of Hydrology and Water Resources, University of Arizona, Tucson, Arizona, U.S.A.*

⁴*Department of Civil Engineering, University of Washington, Seattle, Washington, U.S.A.*

Abstract. We use diagnostic studies of off-line variable infiltration capacity (VIC) model simulations of terrestrial water budgets and 21st-century climate change simulations using the parallel climate model (PCM) to estimate the time required to detect predicted changes in annual precipitation (P), evapotranspiration (E), and discharge (Q) in three sub-basins of the Mississippi River Basin. Time series lengths on the order of 50–350 years are required to detect plausible P , E , and Q trends in the Missouri, Ohio, and Upper Mississippi River basins. Approximately 80–160, 50, and 140–350 years, respectively, are needed to detect the predicted P , E , and Q trends with a high degree of statistical confidence. These detection time estimates are based on conservative statistical criteria ($\alpha = 0.05$ and $\beta = 0.10$) associated with low probability of both detecting a trend when it is not occurring (Type I error) and not detecting a trend when it is occurring (Type II error). The long detection times suggest that global-warming-induced changes in annual basin-wide hydro-climatic variables that may already be occurring in the three basins probably cannot yet be detected at this level of confidence. Furthermore, changes for some variables that may occur within the 21st century might not be detectable for many decades or until the following century – this may or may not be the case for individual recording station data. The long detection times for streamflow result from comparatively low signal-to-noise ratios in the annual time series. Finally, initial estimates suggest that faster detection of acceleration in the hydrological cycle may be possible using seasonal time series of appropriate hydro-climatic variables, rather than annual time series.

1. Introduction

Recent climate predictions for the 21st century warn of increases in global temperature resulting from enhanced concentrations of atmospheric greenhouse gases and aerosols (IPCC, 2001a, b). Temperature increases of the magnitude predicted (1.0–3.5 °C by 2100) could potentially bring about an acceleration in the global water cycle that would lead to increased precipitation, faster evaporation, various changes in streamflow, and a general exacerbation of extreme hydrologic anomalies, such as floods and droughts (Gleick, 1989; Arora and Boer, 2001; Morel, 2001; Nijssen et al., 2001). Warming-induced hydro-climatic changes, if realized, would

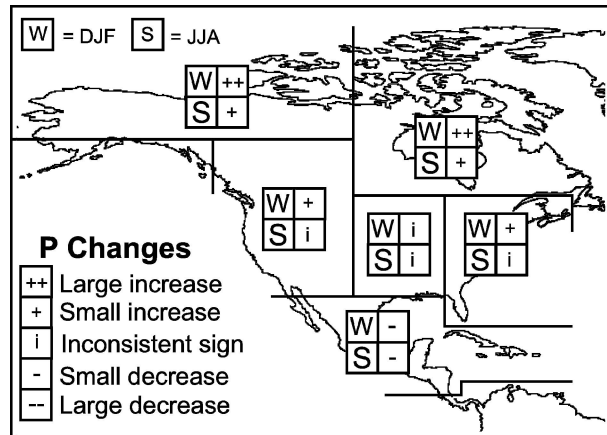


Figure 1. Uncertainty among various model predictions of precipitation (P) changes in North America during the 21st century (adapted from IPCC, 2001c). Predictions are for the IPCC A2 climate change scenario for winter and summer seasons. W refers to the winter months (Dec, Jan, Feb); S, summer months (June, Jul, Aug). A consistent result from at least seven of the nine models included in the IPCC analysis is deemed necessary for agreement. Large increases/decreases exceed $\pm 20\%$; small changes exceed $\pm 5\%$.

likely vary greatly across any one continent. Many climate prediction models, for example, disagree on how hydro-climatic variables in North America would be affected by a warming climate. This is illustrated in Figure 1, which summarizes the uncertainty in model predictions of precipitation across the North American continent during the 21st century. In addition to quantifying the extent to which water balances in various basins will be affected, another question that is important for policymakers is when can changes in hydro-climatic variables such as precipitation (P), runoff (Q), and evapotranspiration (E) be detected. Early detection is critical for minimizing environmental and societal consequences. This is particularly true for large drainages such as the Mississippi River Basin, which comprises 41% of the total land area in the contiguous USA – including important agricultural regions, industrial areas, and population centers within part or all of 31 states.

In a prior work, we estimated for six continents (excluding Antarctica) the number of years needed to detect plausible changes in annual P , E , and Q that might result from warming-induced intensification of the global water cycle (Ziegler et al., 2003). To do so, we examined variance estimates from global-scale water balance simulations using the variable infiltration capacity (VIC) model and trends predicted by the Department of Energy Parallel Community Model (PCM) for a 21st-century, worst-reasonable-case greenhouse gas emission scenario (A2, IPCC, 2001a, b). For the North American continent, predicted trend magnitudes of 0.71, 0.45, and 0.26 mm y^{-1} for P , E , and Q , respectively, require approximately 50, 35, and 75 years to detect with low probability of making either Type I or II errors. At the sub-continent-scale, however, approximately 2–3-fold increases in

TABLE I

A comparison of the following for the North American continent and the Mississippi River Basin (from Ziegler et al., 2003): (i) estimated trends (τ) in precipitation (P), evapotranspiration (E), and residual runoff ($Q = P - E$), as predicted by the parallel climate model (PCM) run B06.20 (IPCC global warming scenario A2); (ii) estimated variances (σ_ε^2) for P , E , and Q , as determined from variable infiltration model (VIC) analyses of terrestrial water balances (Nijssen et al., 2001); and (iii) number of years (y_{detect}) required to detect significantly ($\alpha = 0.05$; $\beta = 0.10$) the predicted trend τ , given the corresponding variance σ_ε^2

Hydro-climatological variable	Statistic	Units	North America	Mississippi Basin
P	τ	mm y ⁻¹	0.71	0.66
	σ_ε^2	mm ²	433	5551
	y_{detect}	years	48	116
E	τ	mm y ⁻¹	0.45	0.78
	σ_ε^2	mm ²	70	1041
	y_{detect}	years	35	60
Q	τ	mm y ⁻¹	0.26	-0.11
	σ_ε^2	mm ²	217	1475
	y_{detect}	years	73	253

time are needed to detect predicted trends in the Mississippi River Basin with the same level of statistical confidence (Table I). This dramatic increase in detection time is largely a function of higher natural variability in the Mississippi River Basin, compared with the continent as a whole. We investigate this issue further in this paper by calculating the time required to detect predicted warming-induced changes in the three largest sub-basins of the Mississippi River: Missouri (MO), Ohio (OH), and Upper Mississippi (UM) River basins.

2. Mississippi River Basin

Beginning in the Lake Itasca region of north-central Minnesota, the Mississippi River flows 3780 km southward to the Gulf of Mexico. Total drainage area of the Mississippi River basin is about 3,200,000 km². The Missouri River, the Ohio River, and the Upper Mississippi form the three largest sub-basins, occupying roughly 1,400,000, 550,000, and 450,000 km², respectively (Figure 2). Beginning in Three Forks, Montana, the Missouri River flows 4370 km to a location near St. Louis, Missouri. It drains approximately 1/6 of the contiguous USA, and roughly 25,000 km² in Canada. The Ohio River begins in Pittsburgh, Pennsylvania, at the junction of the Allegheny and Monongahela Rivers; it then flows about 1560 km to where it joins the Mississippi River at Cairo, Illinois. The Upper Mississippi River basin is defined as the Mississippi River basin upstream of its confluence with the Missouri River.

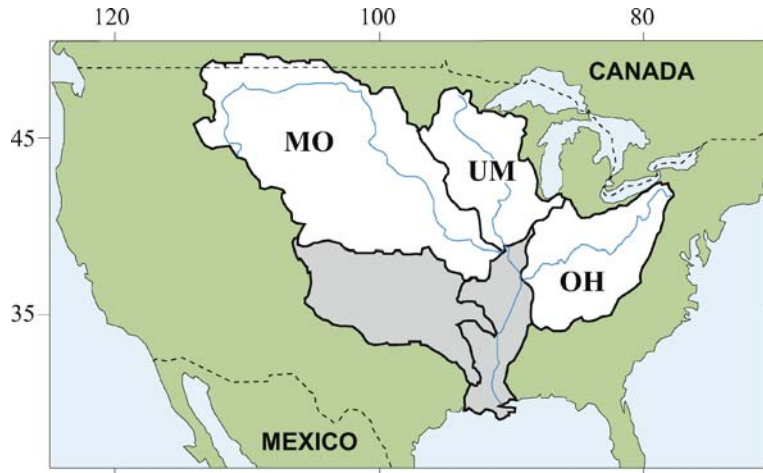


Figure 2. The Missouri (MO), Ohio (OH), and Upper Mississippi (UM) River basins within the Mississippi River Basin, USA. MO, OH, and UM are shaded white; the remainder of the Mississippi River Basin that is not considered in this paper is shaded light gray.

More than 70 million people live in the Mississippi River Basin, one of the world's most productive agriculture regions (e.g., corn, soybeans, wheat, sorghum, livestock, poultry). A majority of all pesticides and fertilizers used in the USA are applied to croplands that are drained by the Mississippi River (USGS, 2003). Water quality in the Mississippi River and Gulf of Mexico is affected by contaminants (e.g., sediment, nutrients, pesticides, trace metals, industrial organic compounds, and sewage) that originate throughout the basin (cf. Goolsby et al., 1997; Meade, 1995). Despite draining more than 60% of the Mississippi Basin, the Missouri River contributes only 42% of the annual flow at St. Louis (USACE, 2003), but it is an important source of sediment. The Ohio River contributes the highest discharge in the Mississippi Basin, but is a relatively small sediment source (USACE, 2003). The Missouri basin is the most highly managed of the three, with a total basin-wide reservoir storage capacity approaching the annual flow volume, and irrigation depletions of nearly 30% of the virgin flow (Solley et al., 1998). This high level of water use and management in all three sub-basins emphasizes the potential impact of hydrologic changes. Changes in the hydrologic cycle will result in changes in the concentrations of contaminants and sediment mobilized and ultimately delivered to the Gulf of Mexico, compounding the effects of hydrologic change.

3. Background

Several studies have attempted to detect contemporary trends in hydro-climatic variables within the continental USA, including regions encompassing the Mississippi River Basin (e.g., Lettenmaier et al., 1994; McCabe and Wolock, 1997; Lins and

Slack, 1999; Karl and Knight, 1998; Milly and Dunne, 2001). For the period 1948–1988, Lettenmaier et al. (1994) found strong season-dependent P and Q trends in some regions: e.g., the strongest P trends were for September–December at as many as 250 stations located mostly in the central part of the country; the strongest Q trends were for November–April in the north-central states region. In another study, Karl and Knight (1998) reported that while the proportion of extreme and heavy precipitation events in the USA increased significantly between 1910 and 1996, a systematic national trend in median precipitation amount was not apparent (cf. Lins and Slack, 1999). Olsen et al. (1999) showed statistically significant stream flow trends at some gauging stations along the Upper Mississippi River (records ranging from 60 to 130 years in length), but found no consistent trend pattern for the Missouri River, the largest tributary of the Mississippi River. In an analysis of water and energy fluxes in the Mississippi River Basin, Milly and Dunne (2001) reported an upward trend in E , which is driven principally by natural increases in P , but also by changes in consumptive water use. In a reassessment of 1957–1988 pan evaporation data, Golubev et al. (2001) reported significant increases (0.01 level) of about 0.8–2.0% per 10 years in actual evaporation in the Midwestern and Great Plains regions of the USA. While analyses of historic data records can assess the significance of detected trends, when examining projected future trends the important issue is not only the trend magnitude *per se*, but the record length required to detect it – which has implications for developing mitigation strategies and designing observational networks.

4. Methods

4.1. TREND DETECTION METHODOLOGY

Our methodology is based on statistical equations that determine the probability (β) of committing a Type II error during one-sample testing for a trend. In hypothesis testing one compares a null hypothesis (H_0 : a trend does not exist) with an alternative hypothesis (H_1 : a trend does exist). The probability of choosing H_0 when H_0 is true is $1 - \alpha$; and the probability of choosing H_1 when H_1 is true is $1 - \beta$. These two probabilities are generally referred to, respectively, as the confidence level of the test and the power of the test. Power, which varies with record length, trend magnitude, and the distribution/form of the time series, is the probability of detecting a specified trend at a fixed confidence level.

The power of the test ($1 - \beta$) for a time series of annual values can be expressed by the following equation (cf. Lettenmaier, 1975):

$$1 - \beta = 1 - F_x \left(W_{1-\alpha/2} - \frac{|\tau_{\min}|}{\text{var}(\hat{\tau})^{1/2}} \right) \quad (1)$$

where F_x is the cumulative normal distribution; $W_{1-\alpha/2}$ is the normal deviate at cumulative probability $1 - \alpha/2$; α is the probability of making a Type I error; τ_{\min}

the minimum detectable trend per year for the time series in question; and $\text{var}(\hat{\tau})$ is the variance of the time series residual computed over n years of observation, calculated as:

$$\text{var}(\hat{\tau}) = \frac{\sigma_{\varepsilon}^2}{\sum_{i=1}^n (t_i - \bar{t})^2} \quad (2)$$

where σ_{ε}^2 is the variance of the ‘noise process’ (assumed to be equal to the sample variance of the time series); each t_i is one year in the record; and \bar{t} is the mean year.

By combining Equations (1) and (2), the number of years (y_{detect}) needed to detect an observed trend (τ) for a specified α and β can be determined by solving for y_{detect} in the left-hand side of the following equation:

$$\sum_{i=1}^{y_{\text{detect}}} (t_i - \bar{t})^2 = \frac{\sigma_{\varepsilon}^2}{\tau^2} (W_{1-\alpha/2} - W_{\beta})^2 \quad (3)$$

where W_{β} is the normal deviate at cumulative probability β ; $W_{1-\alpha/2}$ and σ_{ε}^2 are as above. Herein, estimates of the variance are determined from the VIC model simulations based on observed climate, while trend estimates are based on climate model simulations.

4.2. VARIANCE CALCULATIONS

For each sub-basin and hydro-climatological variable investigated, we calculate σ_{ε}^2 in Equation (3) from 50-year (1950–1999) $1/8^{\circ}$ simulations with the VIC macro-scale hydrological model. VIC (Liang et al., 1994, 1996) has been used in many recent simulations for large river basins (e.g., Abdulla et al., 1996; Cherkauer and Lettenmaier, 1999; Nijssen et al., 1997; Wood et al., 1997, 2002; Maurer et al., 2001). The simulations we use herein are those performed by Maurer et al. (2002). Precipitation forcing consists of observed daily values from the NOAA Cooperative Observer (Co-op) Stations, gridded to the $1/8^{\circ}$ VIC domain using the SYMAP algorithm of Shepard (1984). The long-term averages of the gridded data are scaled to the long-term average of the parameter-elevation regressions on independent slopes model (PRISM) precipitation data set (Daly et al., 1994, 1997) to adjust for any bias introduced by gridding with precipitation stations more densely populated at lower elevations (cf., Widmann and Bretherton, 2000). Prior to gridding temperature data (also from the Co-op station observations), a mean elevation for each VIC cell was calculated by aggregating the topographic information from the Global 30 Arc Second Elevation Data Set (GTOPO30, produced by the US Geological Survey’s EROS Data Center). During gridding, the temperatures were lapsed from each of the neighboring stations to the elevation of the grid cell using a lapse rate of -6.5°C per 1000 m elevation. Wind speed forcing was derived from daily wind data obtained from the NCAR/NCEP reanalysis (Kalnay et al., 1996). Landcover characterization was based on the data described in Hansen et al.

(2000). LAI was derived from the gridded monthly database of Myneni et al. (1997) and indexed to land-cover type as described by Maurer et al. (2002). Soil textures were derived from the data set of Miller and White (1998), which is based on the USDA-NRCS State Soil Geographic Database (STATSGO); specific hydraulic characteristics were inferred using Rawls et al. (1993).

4.3. TREND CALCULATIONS

We use output data from PCM (version 1.1) simulation B06.20 for the 21st century to determine P , E , and Q trends (τ in Equation (3)) for each of the three sub-basins. PCM results from the coupling in parallel of (1) the National Center for Atmospheric Research (NCAR) Community Climate Model version 3 (CCM3) – which includes the NCAR land surface model and soil-vegetation-atmospheric transfer scheme, (2) the Los Alamos National Laboratory Parallel Ocean Program (POP) model, and (3) the sea ice model from the Naval Postgraduate School. Washington et al. (2000) describe PCM and recent simulations. The B06.20 simulation corresponds to ‘global warming’ scenario A2 in recent assessments by the Intergovernmental Panel on Climate Change (IPCC, 2001a, b). Scenario A2 is generally regarded as a worst-reasonable-case scenario, which is characterized by a 4–5-fold increase in CO_2 emissions over the period 2000–2099. During this period, CO_2 concentrations increase from about 350 to over 800 ppm. We first use a bilinear interpolation scheme to convert the PCM P and E fields (Gaussian grid, 128×64 cells, roughly 2.8°) to our $1/8^\circ$ VIC model grid domain (land areas only). We then average the values over the same grid cells used in the VIC terrestrial water balance simulations from which the variances are computed. Values of Q (not available for PCM) are calculated as residual discharge ($Q = P - E$); in this calculation, we assume the year-to-year changes in soil moisture are negligible (cf. Wigley and Jones, 1985).

We calculate trend magnitude as the slope (m) of the Kendall-Theil Robust Line (Theil, 1950) fit through the time series of annual values of length n :

$$y = m \times t + b \quad (4)$$

where

$$m = \text{median} \left(\frac{y_j - y_i}{t_j - t_i} \right) \quad (5)$$

for all years (t) and time series values (y), for $i = 1, 2, \dots, (n - 1)$ and $j = 2, 3, \dots, n$. In Equation (4), b is calculated as:

$$b = y_{\text{median}} - m \times t_{\text{median}} \quad (6)$$

where, t_{median} and y_{median} are, respectively, the median year and the median value in the time series.

4.4. TREND SIGNIFICANCE

To test for trend significance, we use the Mann-Kendall test (Mann, 1945; Kendall, 1975), which has been used often to investigate trends in hydro-climatological signals (Lettenmaier et al., 1994; Mitosek, 1995; Lins and Slack, 1999; Hisdal et al., 2001; Ziegler et al., 2003). The technique tests whether series values tend to increase or decrease as time increases monotonically (cf. Helsel and Hirsch, 1992). For two-sided testing of a series with n values, the null and alternative hypotheses are expressed as:

$$\left. \begin{array}{l} H_0 : \text{prob}[y_j > y_i] = 0.5 \\ H_1 : \text{prob}[y_j > y_i] \neq 0.5 \end{array} \right\} \text{ for all } t_j > t_i \quad (7)$$

where time series values are denoted by y ; t is time in years; i ranges from 1, 2, . . . , $(n - 1)$; and j ranges from 2, 3, . . . , n . Significance can be determined from a test statistic S that measures the monotonic dependence of y on time:

$$S = \sum_{i=1}^{n-1} \sum_{j=i+1}^n \text{SGN}(y_j - y_i) \quad (8)$$

where SGN is a function that returns a value of -1 , 0 , or 1 , which reflects the sign of the expression $y_j - y_i$.

The range of S is therefore $\pm n(n - 1)/2$. To test significance, a statistic (Z_s) that is closely approximated by the standard normal distribution is computed as:

$$Z_s = \begin{cases} \frac{S-1}{\sigma_s} : S > 0 \\ 0 : S = 0 \\ \frac{S+1}{\sigma_s} : S < 0 \end{cases} \quad (9)$$

for which σ_s is calculated as:

$$\sigma_s = \left[\frac{n(n-1)(2n+5) - \sum_{i=1}^n t_i i(i-1)(2i+5)}{18} \right]^{1/2} \quad (10)$$

where t_i is the number of ties of extent i . Note, an alternative test should be used when $n < 10$. The null hypothesis is rejected at significance level α if $|Z_s| > Z_{\text{critical}}$, where Z_{critical} is the value of the standard normal distribution with an exceedance probability of $\alpha/2$. Additional details regarding the Mann-Kendall test are presented elsewhere (e.g., Helsel and Hirsch, 1992).

5. Results

5.1. VARIABILITY IN P , E , AND Q

The boxplots in Figure 3 show the range and central tendency of the 1950–1999 annual time series for P , E , and Q for the three basins. Again, P is based on gridded observed data; and E and Q are computed for each basin from VIC simulation output fields. Ideally, variance estimates should be based on decades to centuries of data, but reliable, complete, lengthy datasets of this nature do not exist for all variables at this resolution. Although, variability could be estimated from P , E , and Q fields extracted from multi-century-long GCM control runs, we favor the VIC-derived values because the P data field is derived from observations and E and Q have been validated for the study area (Maurer et al., 2002). In addition, Maurer et al. (2001) showed that VIC produced more realistic variance estimates than typical GCM runs for mean water cycle elements over the continents. Also lending credibility to the VIC-based approach is Morel's (2001) observation that GCM variances tend to be

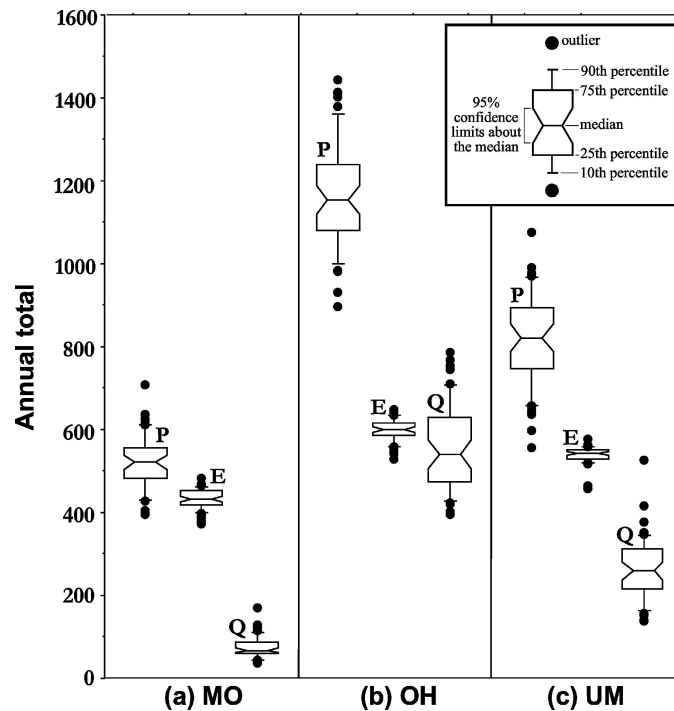


Figure 3. Box plots describing the 1950–1999 precipitation (P), evapotranspiration (E), and discharge (Q) annual time series for the Missouri (MO), Ohio (OH), and Upper Mississippi (UM) River Basins. P is derived from station-based observations; E and Q are VIC water balance simulation output fields. These data are used to calculate the natural variances (σ_{ϵ}^2) for the trend detection estimates (Table II).

TABLE II

For the Missouri (MO), Ohio (OH) and Upper Mississippi (UM) River Basins: (i) means and (ii) corresponding variability (σ_ε^2) of annual precipitation (P) forcing and VIC-simulated annual evapotranspiration (E) and runoff (Q); (iii) coefficients of variation ($C_v = \sigma_\varepsilon/\text{mean}$) for each hydro-climatological variable; (iv) estimated trend magnitudes (τ ; Equation (4)) for the period 2000–2099, predicted by PCM run 06.20 (IPCC global warming scenario A2); (v) the number of years (y_{detect} , Equation (3)) required to detect significantly ($\alpha = 0.05$, $\beta = 0.10$) each τ given the corresponding σ_ε^2

Hydro-climatological variable	Statistic	Units	MO	OH	UM
P	Mean	mm	520	1166	818
	σ_ε^2	mm ²	4495	16872	12325
	C_v	–	0.13	0.11	0.14
	τ	mm y ⁻¹	1.01	0.76	0.59
	y_{detect}	years	82	154	163
E	Mean	mm	433	598	540
	σ_ε^2	mm ²	601	799	477
	C_v	–	0.06	0.05	0.04
	τ	mm y ⁻¹	0.89	1.03	0.77
	y_{detect}	years	46	46	47
Q	Mean	mm	74	558	268
	σ_ε^2	mm ²	707	10793	5516
	C_v	–	0.36	0.19	0.28
	τ	mm y ⁻¹	0.17	–0.3	–0.12
	y_{detect}	years	143	245	353

unrealistically low. Again, the time series summarized in Figure 3 are those used to calculate σ_ε^2 in Equation (3) (Table II). Associated means and the coefficients of variation ($C_v = \sigma_\varepsilon/\text{mean}$) are also reported in Table II. The C_v values indicate that the variability among the three basins is only appreciably different for Q .

5.2. PREDICTED TRENDS IN 21ST-CENTURY P , E , AND Q

Figure 4 shows for each basin and water balance variable the PCM-predicted P , E , and Q trends for 2000–2099 (calculated for the IPCC A2 Scenario). Trend magnitudes (τ) are listed in Table II; associated p -values and powers ($1 - \beta$) for each τ are listed in Table III. Predicted trends for P and E are on the order of 0.6–1.0 mm y⁻¹ in all three basins. The E trends in all three basins and the P trend in MO are highly significant; the OH and UM P trends are significant at 93 and 96% confidence levels ($1 - \alpha$), respectively. The predicted Q trends are variable in both magnitude and sign, but none are significant above a 75% confidence level. MO shows a predicted 0.17 mm y⁻¹ increase in Q , while the OH and UM show

TABLE III

For each of the three basins investigated: (i) trends (τ , Equation (4)) in annual precipitation (P), evapotranspiration (E), and runoff (Q), as predicted in PCM run 06.20 for 2000–2099 (Figure 4); (ii) p -values for the predicted τ ; and (iii) power ($1 - \beta$) values for the predicted τ at $\alpha = 0.05$

	Variable/statistic	Units	MO ^a	OH	UM
P	τ	mm y ⁻¹	1.01	0.76	0.59
	p -value ^b	–	<0.001	0.07	0.04
	$1 - \beta$	–	0.99	0.42	0.46
E	τ	mm y ⁻¹	0.89	1.03	0.77
	p -value ^b	–	<0.001	<0.001	<0.001
	$1 - \beta$	–	>0.99	>0.99	>0.99
Q	τ	mm y ⁻¹	0.17	–0.30	–0.12
	p -value ^b	–	0.32	0.28	0.50
	$1 - \beta$	–	0.14	0.15	0.08

^aMO, OH, and UM are the Missouri, Ohio, and Upper Mississippi River basins.

^bThe p -value is the probability of wrongly rejecting H_0 if H_0 is true; if it is less than the chosen significance level the trend is significant.

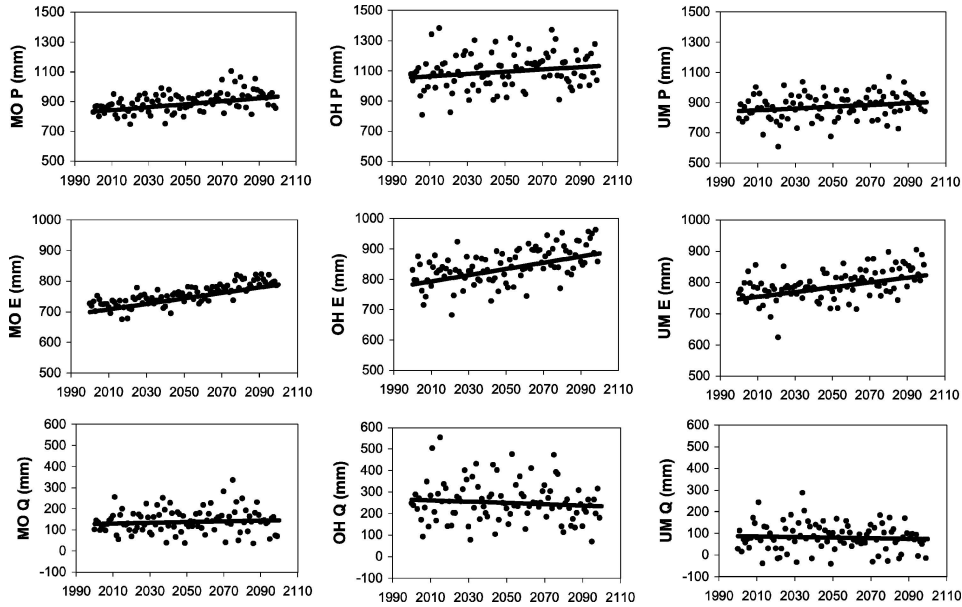


Figure 4. Predicted trends in precipitation (P), evapotranspiration (E), and residual discharge ($Q = P - E$) for the Missouri (MO), Ohio (OH), and Upper Mississippi (UM) River Basins. Time series data are from PCM simulations of the IPCC A2 21st century climate change scenario. The slope of the line (Equation (4)) is the predicted trend (τ) used in the trend detection estimates (Table II).

decreases of 0.30 and 0.12 mm y^{-1} . Other studies have similarly reported decreases in long-term mean streamflow for warmer climate scenarios, while simulated effects on other streamflow statistics (e.g., flood peaks) are variable (e.g., Arora and Boer, 2001; Nijssen et al., 2001; Evans and Schreider, 2002).

5.3. DETECTION TIME

The number of years (y_{detect}) required to detect the PCM-predicted trends for each basin are listed in Table II. These values are based on conservative criteria for committing Type I and II errors ($\alpha = 0.05$, $\beta = 0.10$, respectively). Again, y_{detect} is computed via Equation (3) from the VIC-derived variances (σ_{ϵ}^2) and PCM-derived trends (τ), which are also listed in Table II. The following basin ordering applies regarding time to detect trends in all three variables: MO < OH < UM. Detection time is lowest for predicted evapotranspiration changes; and is less than 50 years in all sub-basins. Annual time series on the order of 80–160 years are needed to detect predicted precipitation changes, with detection for OH (154 years) being intermediate of that for MO (82 years) and UM (163 years). In comparison with P and E , y_{detect} values are long for Q : approximately 140, 250, and 350 years for MO, OH, and UM, respectively.

6. Discussion

Few analyses to date have confirmed that contemporary hydro-climatic trends in the area of the Mississippi River Basin result from climate change. Olsen et al. (1999) stated that anthropogenic climate change was the least likely cause of the observed upward trends in the Upper and Lower Mississippi River flows. Lettenmaier et al. (1994) concluded that the stream flow trends they identified were not entirely consistent with changes in climate, but may have been related to a combination of climate and water management effects. The climate model studies conducted by Milly and Dunne (2001) support that only a very small contribution to the P increases in the Mississippi Basin could be attributed to changes in greenhouse gases and aerosols.

For all three variables the annual trend is small compared with the annual variance, which results in a low signal-to-noise ratio. This exacerbates the problem posed by water management practices, and makes it more difficult to establish whether a trend in any hydro-climatic record is statistically significant. This was demonstrated by McCabe and Wolock (1997) in their examination of annual stream flow records for 585 US basins with drainage areas ≤ 2500 km². They determined there was only an average probability of 28% for detection of a 20% increase in annual runoff over a 100-year period (at a confidence level at 95%). Low probability was, in part, associated with low ratios of mean annual runoff to the standard deviation of annual runoff. Figure 5 shows the general relationship between detection

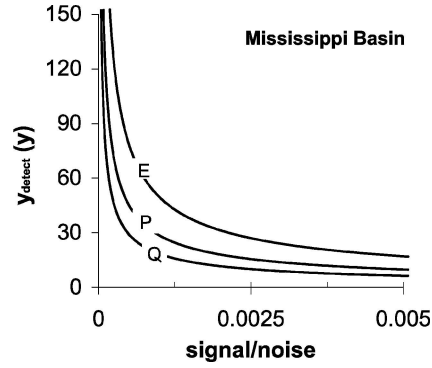


Figure 5. Influence of the signal-to-noise ratio on calculated detection time (y_{detect} , Equation (3); $\alpha = 0.05$, $\beta = 0.10$) for precipitation (P), evapotranspiration (E), and discharge (Q) in the Mississippi River Basin (based on data in Ziegler et al., 2003). Signal-to-noise ratio is calculated as $\tau/\sigma_{\varepsilon}^2$, where σ_{ε}^2 is the value reported in Table I, and trend magnitude (τ) varies over several orders of magnitude.

time and the signal-to-noise ratio for P , E , and Q in the entire Mississippi River Basin. Important in the figure is that as the signal-to-noise ratio approaches zero, detection time increases rapidly.

The smallest detection times for the MO, OH, and UM sub-basins by far are for E , for which σ_{ε}^2 values are similarly low and predicted τ magnitudes are relatively high. However, in comparison with P and Q (observed in its integrated form as streamflow), E is sparsely measured and difficult to determine through observations. In the USA, multi-decadal records of pan evaporation exist at fewer than 500 locations (compared with approximately 7000 P observation sites). In evaluating trends, the relationship between pan evaporation and terrestrial evaporation has been shown to be the inverse, further complicating the use of pan evaporation data (Peterson et al., 1995; Brutsaert and Parlange, 1998; Lawrimore and Peterson, 2000; also see Golubev et al., 2001). For these reasons, evapotranspiration at this scale is typically modeled or determined indirectly (e.g., Milly and Dunne, 2001). Because measurement errors associated with the determination of E are difficult to quantify, their influence on σ_{ε}^2 and t calculations is particularly uncertain.

Simply stated, α in Equation (3) is the probability of detecting intensification when there is none; and β is the probability of not detecting intensification when it is occurring. In addition to the variance and trend magnitudes used in the calculation, specified values of α and β directly determine y_{detect} . Because our detection time calculations are based on low probabilities for making errors (i.e., $\alpha = 0.05$ and $\beta = 0.10$), the seemingly long y_{detect} values reported in Table II represent a ‘low risk’ assessment. The curves shown in Figure 6 demonstrate how detection time decreases for increasing values of α and β (i.e., higher risk and greater uncertainty). As shown for each basin and hydro-climatic variable, the larger the values of α and β , the shorter the time needed to detect the predicted trends significantly. Of note in the figure is that even with a relatively high-risk assessment (i.e., $\alpha = \beta = 0.5$),

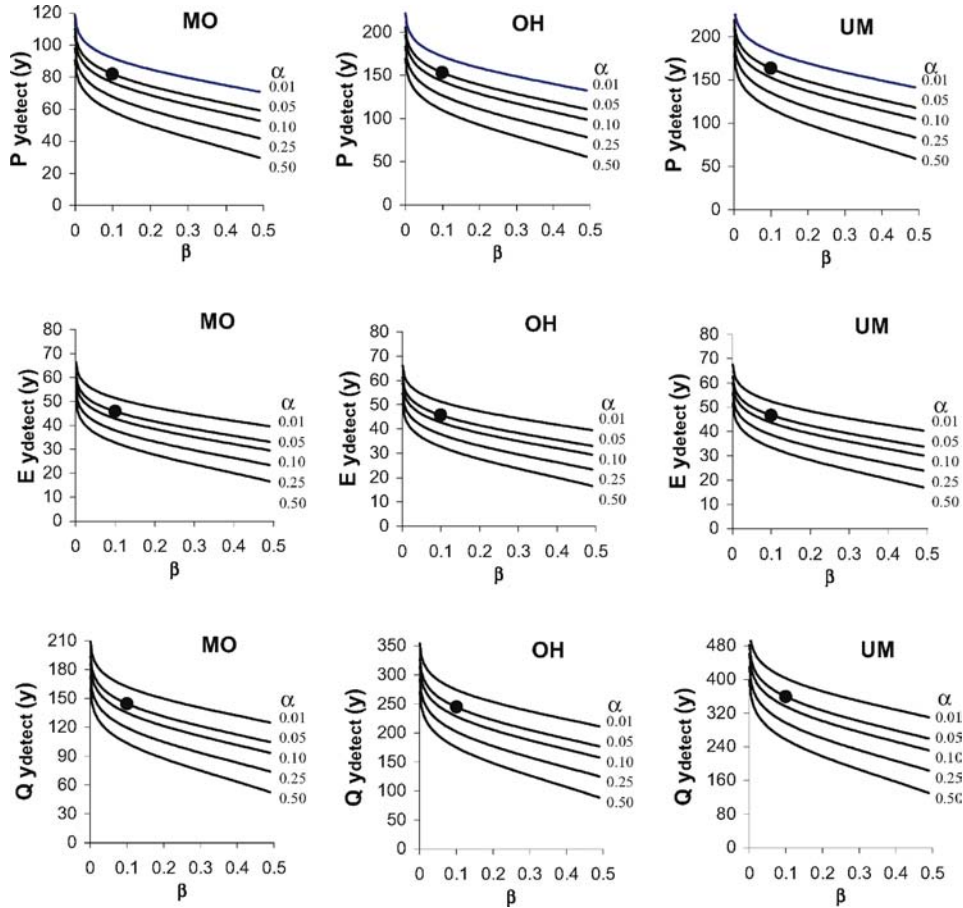


Figure 6. Estimated detection times (y_{detect}) at various degrees of statistical confidence for each hydro-climatological variable (precipitation (P), evapotranspiration (E), and discharge (Q)) within the Missouri (MO), Ohio (OH), and Upper Mississippi (UM) River Basins. The parameters α and β are, respectively, the probabilities of making Type I and II errors in testing (Equation (1)). The closed circles indicate the y_{detect} estimates ($\alpha = 0.05$, $\beta = 0.10$) presented in Table II.

long time series are still needed to detect significantly the Q changes in all basins.

Our long detection times do not necessarily represent minimum detection times, as they are based on predicted trends of one climate model simulating the A2 global change scenario. Just as there are many prediction models, there are several global-change scenarios, each resulting in a unique temperature time series. For example, the various scenarios investigated by the IPCC (Chapter 9, Figure 9.14, 2001b) produce a temperature-increase envelope ranging from roughly 1.5–6 °C. Similarly, these scenarios produce a range of plausible trends in 21st-century P , E , and Q – some being larger in magnitude than those used herein; others lower.

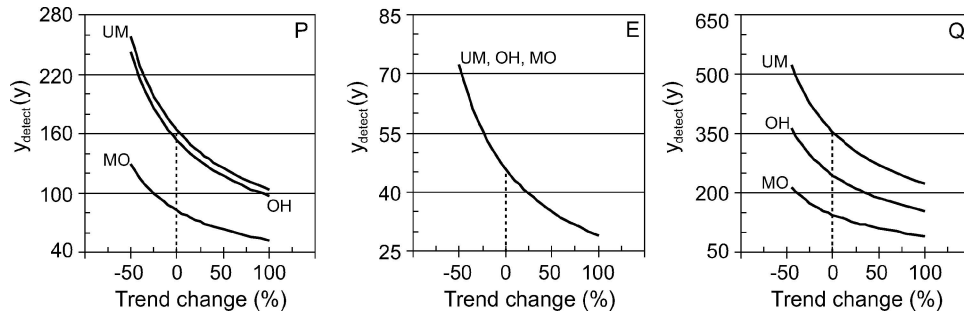


Figure 7. For each sub-basin and annual precipitation (P), evapotranspiration (E), and residual discharge ($Q = P - E$), changes in detection time (y_{detect} , Equation (3)) for trend magnitudes ranging from 50% weaker to 100% stronger than those predicted by PCM for the A2 scenario (i.e., 0% change; dotted line).

Figure 7 shows differences in detection time for both weaker and stronger trends than those we used in the calculations of y_{detect} shown in Table II. Even if P and Q trend magnitudes are twice those predicted by PCM for the A2 scenario, detection is only possible in one basin (MO) using data records that are shorter than about 100 years. This result is comparable to what McCabe and Wolock (1997) found for discharge in smaller basins.

Finally, it is likely that annual time series are not the most sensitive indicators of hydrological acceleration. In some regions, seasonal signals may allow for quicker detection times if hydrological acceleration manifests itself as an increase in the frequency of extreme events. In support, Karl and Knight (1998) found that precipitation increases in the USA during the 20th century were most pronounced in spring and autumn seasons, but were also apparent in the summer season. The y_{detect} values in Table IV show that in comparison with their corresponding annual time series, detectability of predicted changes in precipitation varies widely among the winter (DJF), spring (MAM), summer (JJA), and autumn (SON) seasons. For some seasons, detection time is as little as one-third to one-half of that determined using the annual time series. For the MO and UM basins, both of which exhibit a marked seasonal cycle, the season with the shortest detection time is also the driest season, DJF. The OH basin, which has a much less pronounced seasonal P cycle, shows the shorter trend detection times in the wetter months (MAM and JJA). MAM shows the greatest increasing (positive) trend in all basins, and shorter detection times than JJA and SON. Detection time in all three basins was lower than that for the annual time series for at least two seasonal series. In the case of UM, all four seasonal time series facilitated quicker detection times than the annual time series, due to a sharp declining P trend in the DJF, and increasing trends all other seasons. These initial results using P demonstrate the advantages of looking at seasonal versus annual data for detecting trends related to acceleration in the hydrologic cycle.

TABLE IV

For each of the three basins investigated: (i) mean and variance (σ_ϵ^2) of seasonal precipitation (P); (ii) trends (τ , Equation (4)) in seasonal precipitation, as simulated by the parallel climate model (PCM) run B06.20 (IPCC global warming scenario A2); and (iii) the estimated years (y_{detect} , Equation (3)) to detect significantly ($\alpha = 0.05$, $\beta = 0.10$) each τ given the corresponding σ_ϵ^2

Basin	Season	Mean (mm)	σ_ϵ^2 (mm ²)	τ (mm y ⁻¹)	y_{detect} (years)
MO ^a	DJF	56	104	0.40	44
	MAM	161	832	0.73	58
	JJA	197	1486	0.45	98
	SON	108	1026	0.44	87
OH	DJF	279	7294	0.35	195
	MAM	326	3297	0.56	109
	JJA	315	2387	-0.36	131
	SON	254	3706	-0.08	423
UM	DJF	93	1875	-1.21	54
	MAM	224	2137	0.89	70
	JJA	314	3317	0.39	138
	SON	195	3874	0.54	118

^aMO, OH, and UM are the Missouri, Ohio, and Upper Mississippi River basins; seasons DJF, MAM, JJA, SON correspond to the three-month periods December–February, March–May, June–August, and September–November.

7. Conclusion

Our analyses indicate that for the three largest sub-basins of the Mississippi River times series on the order of 50 years to a few centuries are needed to detect plausible basin-wide changes in annual precipitation, evaporation, and discharge that may result from anthropogenic warming. Specifically for the Missouri, Ohio, and Upper Mississippi River Basins, predicted changes in annual P , E , and Q require roughly 80–160, 50, and 140–350 years to detect with high confidence. These estimates are based on the following: (1) the natural variance in P , E , and Q , as determined from diagnostics simulations using the VIC model; (2) PCM-estimated trends in P , E , and residual Q for the 21st century (simulated for the IPCC global warming scenario A2); and (3) low-risk criteria for committing Type I ($\alpha = 0.05$) and Type II errors ($\beta = 0.10$). These long detection time estimates suggest that even using the longest available records, we may not yet be able to detect basin-wide hydroclimatic changes that have taken place up to now – although this might not be true for P at some scales or for individual recording stations where the signal-to-noise ratio is higher (cf. Morel, 2001). For some variables, particularly streamflow, we likely cannot detect realized changes significantly before the end of the 21st century – not even if the observed trends are twice the magnitude of those estimated by the PCM for the A2 scenario. Quicker detection times can be generated using higher-risk

statistical criteria, but even in doing so, detection times for streamflow would still be on the order of 60–120 years in the three basins. Finally, quicker detection may be possible using seasonal time series and/or using other types of variables that are direct hydro-climatic indicators of changes in extreme events (e.g., variables related to precipitation amount, frequency, and intensity, as in Karl and Knight, 1998).

With each passing year of observation, the variability and trend magnitudes change, thereby increasing or decreasing y_{detect} . However, barring a dramatic hydro-climatic change, or relaxation of the criteria to detect a trend with significance, high-confidence detection of plausible warming-induced changes may not be feasible for some time to come. As stated by McCabe and Wolock (1997), the physical importance of a trend, even one that has not been deemed statistically significant, is that it may have important effects on water resources. Furthermore, waiting for unequivocal proof of hydrological cycle acceleration before instituting policies to address potential causes may turn out to be excessively detrimental to vulnerable populations.

Acknowledgments

This work is supported by NASA grants NAG5-9414, NAG5-9886. PCM data were downloaded with permission from the UCAR website (<http://www.cgd.ucar.edu/pcm/>). A special thanks to Ross A. Sutherland for tying up some loose ends in the notation.

References

- Abdulla, F. A., Lettenmaier, D. P., Wood, E. F., and Smith, J. A.: 1996, 'Application of a macroscale hydrologic model to estimate the water balance of the Arkansas-Red River Basin', *J. Geophys. Res.* **101**, 7449–7459.
- Arora, V. K. and Boer, G. J.: 2001, 'Effects of simulated climate change on the hydrology of major river basins', *J. Geophys. Res.* **106**(D4), 3335–3348.
- Brutsaert, W. and Parlange, M. B.: 1998, 'Hydrologic cycle explains the evaporation paradox', *Nature* **396**, 30.
- Cherkauer, K. A. and Lettenmaier, D. P.: 1999, 'Hydrologic effects of frozen soils in the upper Mississippi River basin', *J. Geophys. Res.* **104**(D16), 19,599–19,610.
- Daly, C., Neilson, R. P., and Phillips, D. L.: 1994, 'A statistical-topographic model for mapping climatological precipitation over mountainous terrain', *J. Appl. Meteorol.* **33**, 140–158.
- Daly, C., Taylor, G. H., and Gibson, W. P.: 1997, 'The PRISM approach to mapping precipitation and temperature', *Reprints: 10th Conference on Applied Climatology*, Reno, NV, American Meteorological Society, pp. 10–12.
- Evans, J. and Schreider, S.: 2002, 'Hydrological impacts of climate change on inflows to Perth, Australia', *Clim. Change* **55**(3), 361–393.
- Gleick, P. H.: 1989, 'Climate change, hydrology, and water resources', *Rev. Geophys.* **27**, 329–344.

- Golubev, V. S., Lawrimore, J. H., Groisman, P. Y., Speranskaya, N. A., Zhuravin, S. A., Menne, M. J., Peterson, T. C., and Malone, R. W.: 2001, 'Evaporation changes over the contiguous United States and the former USSR: A reassessment', *Geophys. Res. Lett.* **28**(13), 2665–2668.
- Goolsby, D. A., Battaglin, W. A., and Hooper, R. P.: 1997, 'Sources and transport of nitrogen in the Mississippi River Basin', <http://wwwrcolka.cr.usgs.gov/midconherb/st.louis.hypoxia.html> (downloaded January 2003).
- Evans, J. and Schreider, S.: 2002, 'Hydrological impacts of climate change on inflows to Perth, Australia', *Clim. Change* **55**(3), 361–393.
- Hansen, M. C., DeFries, R. S., Townshend, J. R. G., and Sohlberg, R.: 2000, 'Global land cover classification at 1 km spatial resolution using a classification tree approach', *Int. J. Remote Sens.* **21**(6), 1331–1464.
- Helsel, D. R. and Hirsch, R. M.: 1992, *Statistical Methods in Water Resources*, Elsevier, Amsterdam, 522 p.
- Hisdal, H., Stahl, K., Tallaksen, L. M., and Demuth, S.: 2001, 'Have streamflow droughts in Europe become more severe or frequent?' *Int. J. Climatol.* **21**, 317–333.
- IPCC: 2001a, 'Climate change 2001: Impacts, adaptation & vulnerability', in McCarthy, J. J., Canziani, O. F., Leary, N. A., Dokken, D. J., and White, K. S. (eds.), *Contribution of Working Group II to the Third Assessment Report of the Intergovernmental Panel on Climate Change (IPCC)*, Cambridge University Press, 1032 p.
- IPCC: 2001b, 'Climate change 2001: The scientific basis', in Houghton, J. T., Ding, Y., Griggs, D. J., Noguera, M., van der Linden, P. J., Dai, X., Maskell, K., and Johnson, C. A. (eds.), *Contribution of Working Group I to the Third Assessment Report of the Intergovernmental Panel on Climate Change (IPCC)*, Cambridge University Press, Cambridge, UK, 881 p.
- Karl, T. R.: 1998, 'Regional trends and variations of temperature and precipitation', in Watson, R. T., et al. (eds.), *The Regional Impacts of Climate Change, as Assessment of Vulnerability*, Cambridge University Press, pp. 411–425.
- Karl, T. R. and Knight, R. W.: 1998, 'Secular trends of precipitation amount, frequency, and intensity in the United States', *Bull. Am. Meteorol. Soc.* **79**(2), 231–241.
- Kalnay, E., Kanamitsu, M., Kistler, R., Collins, W., Deaven, D., Gandin, L., Iredell, M., Saha, S., et al.: 1996, 'The NCEP/NCAR 40-year reanalysis project', *Bull. Am. Meteorol. Soc.* **77**, 437–471.
- Kendall, M. G.: 1975, *Rank Correlation Methods*, Charles Griffin, London, 202 p.
- Lawrimore, J. H. and Peterson, T. C.: 2000, 'Pan evaporation trends in dry and humid regions of the United States', *J. Hydrometeorol.* **1**, 543–546.
- Lettenmaier, D. P.: 1975, 'Detection of trends in water quality data from records with dependent observations', *Water Resour. Res.* **12**(5), 1037–1046.
- Lettenmaier, D. P., Wood, E. F., and Wallis, J. R.: 1994, 'Hydro-climatological trends in the continental United States, 1948–88', *J. Clim.* **7**, 586–607.
- Liang, X., Lettenmaier, D. P., and Wood, E. F.: 1996, 'One-dimensional statistical dynamic representation of subgrid spatial variability of precipitation in the two-layer variable infiltration capacity model', *J. Geophys. Res.* **101**, 21,403–21,422.
- Liang, X., Lettenmaier, D. P., Wood, E. F., and Burges, S. J.: 1994, 'A simple hydrologically based model of land surface water and energy fluxes for general circulation models', *J. Geophys. Res.* **99**, 14,415–14,428.
- Lins, H. F. and Slack, J. R.: 1999, 'Streamflow trends in the United States', *Geophys. Res. Lett.* **26**(2), 227–230.
- Mann, H. B.: 1945, 'Nonparametric test against trend', *Econometrica* **13**, 245–259.
- Maurer, E. P., O'Donnell, G. M., Lettenmaier, D. P., and Roads, J. O.: 2001, 'Evaluation of the land surface water budget in NCEP/NCAR and NCEP/DOE reanalyses using an off-line hydrologic model', *J. Geophys. Res.* **106**(D16), 17,841–17,862.

- Maurer, E. P., Wood, A. W., Adam, J. C., Lettenmaier, D. P., and Nijssen, B.: 2002, 'A long-term hydrologically-based data set of land surface fluxes and states for the conterminous United States', *J. Clim.* **15**(22), 3237–3251.
- McCabe, G. J. Jr. and Wolock, D. M.: 1997, 'Climate change and the detection of trends in annual runoff', *Clim. Res.* **8**, 129–134.
- Meade, R. H.: 1995, 'Contaminants in the Mississippi River', USGS Circular 1133, 140 p.
- Miller, D. A. and White, R. A.: 1998, 'A conterminous United States multi-layer soil characteristics data set for regional climate and hydrology modeling', *Earth Interactions* **2**, 1–15.
- Milly, P. C. D. and Dunne, K. A.: 2001, 'Trends in evapotranspiration and surface cooling in the Mississippi River Basin', *Geophys. Res. Lett.* **28**(7), 1219–1222.
- Mitosek, H. T.: 1995, 'Climate variability and change within the discharge time series: A statistical approach', *Clim. Change* **29**, 101–116.
- Morel, P.: 2001, 'Why GEWEX? The agenda for a global energy and water cycle research program', in Twitchell, P. (ed.), *GEWEX NEWS* 11(1), 1,7–11, International GEWEX Project Office, 1010 Wayne Avenue 450, Silver Spring, MA, USA.
- Myneni, R. B., Nemani, R. R., and Running, S. W.: 1997, 'Estimation of global leaf area index and absorbed PAR using radiative transfer models', *IEEE Trans. Geosci. Remote Sens.* **35**(6), 1380–1393.
- Nijssen, B., Lettenmaier, D. P., Liang, X., Wetzel, S. W., and Wood, E. F.: 1997, 'Streamflow simulation for continental-scale river basins', *Water Resour. Res.* **33**, 711–724.
- Nijssen, B., O'Donnell, G. M., Hamlet, A. F., and Lettenmaier, D. P.: 2001, 'Hydrologic sensitivity of global rivers to climate change', *Clim. Change* **50**(1–2), 143–175.
- Olsen, J. R., Stedinger, J. R., Matalas, N. C., and Stakhiv, E. Z.: 1999, 'Climate variability and flood frequency estimation for the Upper Mississippi and Lower Mississippi Rivers', *J. Am. Water Resour. Assoc.* **35**(6), 1509–1523.
- Peterson, T. C., Golubev, V. S., and Groisman, P. Y.: 1995, 'Evaporation losing its strength', *Nature* **377**, 687–688.
- Rawls, W. J., Ahuja, L. R., Brakensiek, D. L., and Shirmohammadi, A.: 1993, 'Infiltration and soil water movement', in Maidment, D. (ed.), *Handbook of Hydrology*, pp. 5.1–5.51.
- Shepard, D. S.: 1984, 'Computer mapping: The SYMAP interpolation algorithm', in Gaile, G. L. and Willmott, C. J. (eds.), *Spatial Statistics and Models*, D. Reidel Publishing Co., pp. 133–145.
- Solley, W. B., Pierce, R. R., and Perlman, H. A.: 1998, 'Estimated use of water in the United States in 1995', USGS Circular 1200.
- Theil, H.: 1950, 'A rank-invariant method of linear and polynomial regression analysis', *Indagationes Math.* **12**, 85–91.
- USACE: 2003, United States Army Corps of Engineers, download date: January, 2003, <http://www.mvr.usace.army.mil/PublicAffairsOffice/HistoricArchives/>.
- USGS: 2003, United States Geological Survey, <http://water.usgs.gov/nasqan/missfact/msfact.html>, download date: January, 2003.
- Washington, W. M., Weatherly, J. W., Meehl, G. A., Semtner, A. J., Jr., Bettge, T. W., Craig, A. P., Strand, W. G. Jr., Arblaster, J., Wayland, V. B., James, R., and Zhang, Y.: 2000, 'Parallel climate model (PCM) control and transient simulations', *Clim. Dynam.* **16**(10/11), 755–774.
- Widmann, M. and Bretherton, C. S.: 2000, 'Validation of mesoscale precipitation in the NCEP re-analysis using a new grid-cell data set for the northwestern United States', *J. Clim.* **13**, 1936–1950.
- Wigley, T. M. L. and Jones, P. D.: 1985, 'Influences of precipitation changes and direct CO₂ effects on streamflow', *Nature* **314**, 149–152.
- Wood, A. W., Maurer, E. P., Kumar, A., and Lettenmaier, D. P.: 2002, 'Long range experimental hydrologic forecasting for the eastern U.S.', *J. Geophys. Res.*, **107**(D20), 4429 (doi:10.1029/2001JD000659).

- Wood, E. F., Lettenmaier, D. P., Liang, X., Nijssen, B., and Wetzel, S. W.: 1997, 'Hydrological modeling of continental-scale basins', *Annu. Rev. Earth Planet. Sci.* **25**, 279–300.
- Ziegler, A. D., Sheffield, J., Maurer, E. P., Nijssen, B., Wood, E. F., and Lettenmaier, D. P.: 2003, 'Detection of intensification of continental-scale hydrological cycles: Temporal scale of evaluation', *J. Clim.* **16**(3), 535–547.

(Received 21 June 2003; accepted in revised form 5 October 2004)